Please cite the Published Version

Hallsworth, Erik Christopher, Augusthus-Nelson, Levingshan, Davis, Sergio, Teklemariam, Aron , Tosheva, Lubomira and Tedesco, Silvia (2025) Calcium Oxide—Rich Industrial Waste Ash as a Lime Substitute in Sustainable Metakaolin—Based Binders. Waste and Biomass Valorization. ISSN 1877-2641

DOI: https://doi.org/10.1007/s12649-025-03386-x

Publisher: Springer

Version: Published Version

Downloaded from: https://e-space.mmu.ac.uk/642728/

Usage rights: Creative Commons: Attribution 4.0

Additional Information: This is an open access article published in Waste and Biomass Valoriza-

tion, by Springer.

Enquiries:

If you have questions about this document, contact openresearch@mmu.ac.uk. Please include the URL of the record in e-space. If you believe that your, or a third party's rights have been compromised through this document please see our Take Down policy (available from https://www.mmu.ac.uk/library/using-the-library/policies-and-guidelines)

ORIGINAL PAPER



Calcium Oxide-Rich Industrial Waste Ash as a Lime Substitute in Sustainable Metakaolin-Based Binders

Erik Christopher Hallsworth 1 • Levingshan Augusthus-Nelson • Sergio Davies • Aron Teklemariam • Lubomira Tosheva • Silvia Tedesco • Silvia T

Received: 3 June 2025 / Accepted: 27 October 2025 © The Author(s) 2025

Abstract

Corrugated cardboard fly ash (CCFA) is an industrial by-product typically sent to landfill. Unlike conventional coal fly ash, CCFA has limited pozzolanic activity but contains a high amount of calcium oxide (CaO). When hydrated, CaO forms calcium hydroxide (Ca(OH)₂), which can react with metakaolin (MK)—a highly reactive aluminosilicate—to promote pozzolanic activation. This makes CCFA a promising material for sustainable cementitious binders. The chemical, physical, and microstructural characteristics of raw and hydrated materials were assessed using mechanical testing, XRF, XRD and BET. Compressive strength development was analysed via response surface methodology across varying water-to-cement ratios. While CCFA alone reduced strength, binary systems replacing 40% of cement with 20% CCFA and 20% MK achieved compressive strengths comparable to mixes with 20% MK alone. These results highlight the potential of CCFA as a sustainable calcium source in low-carbon binder systems, contributing to waste valorisation and cement reduction.

Keywords Calcium oxide-rich waste ash · Characterisation of corrugated cardboard fly ash · Compressive strength · Limemetakaolin blended mortar

- ☐ Erik Christopher Hallsworth erik.c.hallsworth@stu.mmu.ac.uk
- Levingshan Augusthus-Nelson
 L.AugusthusNelson@salford.ac.uk

Sergio Davies Sergio.Davies@mmu.ac.uk

Aron Teklemariam
A.Teklemariam@mmu.ac.uk

Lubomira Tosheva

L.Tosheva@mmu.ac.uk Silvia Tedesco

S.Tedesco1@salford.ac.uk

Published online: 18 November 2025

- Faculty of Science and Engineering, Manchester Metropolitan University, Manchester M1 5GD, UK
- School of Science, Engineering and Environment, University of Salford, Salford M5 4WT, UK
- ³ Centre for Sustainable Innovation, Salford Business School, University of Salford, Salford M5 4WT, UK

Introduction

The global corrugated packaging market has experienced substantial growth in recent years, driven by the expansion of e-commerce, the rising demand for sustainable packaging solutions, and advancements in digital printing technologies. In 2023, the global corrugated cardboard market was valued at \$4.4 billion and is projected to reach \$5.5 billion by 2030 [1]. Although the vast majority of cardboard is recycled, a proportion is non–recyclable due to contamination, composite packaging or physical degradation. As the cardboard industry grows, so does the volume of non–recyclable cardboard. In such cases where recycling is not available, energy recovery of the cardboard sludge through combustion is considered a more feasible alternative to landfilling [2]. However, incineration generates ash, posing ongoing challenges for sustainable waste management.

The incineration of non-recyclable cardboard sludge produces a calcium oxide-rich fly ash known as corrugated cardboard fly ash (CCFA). Unlike traditional fly ashes, CCFA lacks established reuse pathways and is often landfilled, placing additional strain on waste management systems. Despite the United Kingdom achieving a 70.6% recycling



rate for its 5.4 million tonnes of annual paper and cardboard production [3], the handling of fly ash from sludge incineration remains an unresolved issue. While combustion enables energy recovery, it yields fly ash requiring specialised treatment, with limited opportunities for beneficial reuse [4, 5].

Traditionally, fly ash from coal combustion has been widely used as a supplementary cementitious material (SCM) in concrete, valued for its pozzolanic properties that improve strength and durability while reducing Portland cement consumption—a major source of carbon emissions [6–9]. Similar work has been completed using waste paper sludge ash (WPSA) to investigate the role as a potential pozzolan [10]. However, not all fly ashes possess these beneficial characteristics.

The CCFA examined in this study is chemically distinct from conventional coal-derived fly ashes and WPSA. Rich in calcium oxide and exhibiting limited pozzolanic activity, CCFA more closely resembles quicklime than Class F fly ash, Class C fly ash and WPSA, which typically contain significant amounts of silicon dioxide (SiO₂) and aluminium oxide (Al₂O₃) [11]. Upon hydration, the CaO in CCFA forms calcium hydroxide (Ca(OH)₂), which—if left unreacted does not contribute to compressive strength and may even be detrimental. However, in the presence of reactive silicon dioxide and aluminium oxide, this calcium hydroxide can form calcium silicate hydrate and calcium alumino silicate hydrate gels (C-S-H and C-A-S-H) which improve compressive strength by hardening and reducing pore connectivity. This fundamental difference necessitates a reevaluation of CCFA's role in cementitious systems.

Rather than acting as a pozzolan, CCFA may serve as a calcium source, analogous to lime in traditional lime-pozzolan mortars and concretes [12–14]. Traditional pozzolans such as metakaolin [15-17], coal fly ash [18, 19], and ground granulated blast-furnace slag (GGBFS) [18] have been extensively studied for this purpose due to their high SiO₂+Al₂O₃ content. More recently, attention has shifted to industrial and agricultural wastes such as wood fly ash [20], recycled brick dust [21, 22], and glass powder [23, 24]. These studies confirm that materials rich in reactive aluminosilicates can successfully react with lime to improve strength and durability. However, in nearly all cases, waste materials have been used as the pozzolanic component, not as a calcium source. The present work is distinct in that it evaluates a calcium oxiderich waste material, CCFA, as the primary calcium donor, analogous to lime, in a binary system with metakaolin.

Given these properties, CCFA represents an underexplored opportunity. Although unsuitable as a standalone cement substitute, its high calcium oxide content suggests it could be synergistically combined with a reactive pozzolan. This study investigates the potential of blending CCFA with metakaolin—a highly reactive aluminosilicate—to complement CCFA's calcium oxide-rich composition. By pairing

these materials, this research explores the performance of mortar formulations incorporating CCFA as a partial cement replacement, with the aim of developing more sustainable construction materials and contributing to the decarbonisation of the built environment.

Materials

Ordinary Portland Cement (OPC) used in this study was CEM I 52.5R, supplied by Blue Circle Industries, UK. The cement conforms to BS EN 197-1:2011 [25] standards and exhibits consistent chemical composition and mechanical performance.

CCFA was obtained as a by-product of waste corrugated cardboard incineration carried out at approximately 950°C. The ash was collected a commercial paper recycling facility located in Greater Manchester, UK. To ensure experimental consistency for all the samples tested, CCFA was sourced from a single incineration batch and stored in sealed containers within a desiccator to minimise moisture uptake and carbonation. Prior to testing, the ash was homogenised to reduce intra-batch variability by using a mechanical shaker. X-ray fluorescence (XRF) analysis confirmed a high calcium oxide content, with minor variation (±2% CaO) observed across replicate samples. While this study utilised a single, well-characterised batch, the potential for compositional variability in CCFA due to feedstock heterogeneity and combustion efficiency is acknowledged, and future studies should address this in greater depth.

Metakaolin (MK) (Metakaolin Brut, Argical-M 1000, MK-36) was sourced from Imerys Refractory Minerals, Clérac, France. It was used as received and stored in an airtight container under dry conditions to prevent premature hydration. This MK is supplied as a fine, amorphous powder with negligible water solubility and consistent particle size, suitable for use as a high-reactivity pozzolan.

The chemical and physical properties of these materials were characterised using a combination of XRF, X-ray diffraction (XRD), particle size distribution and BET surface area analysis.

Material Characterisation

X-Ray Fluorescence (XRF) Analysis

X-ray fluorescence (XRF) analysis was conducted to assess the chemical composition of the CCFA, OPC, and MK loose powder samples, using a Rigaku NEX-CG energy dispersive X-ray fluorescence spectrometer; results are shown in Table 1. CCFA does not meet the criteria for BS 8615-1:2019 [26] classification as a pozzolanic material due to



Table 1 Chemical compositions by weight percentage of Corrugated Cardboard Fly Ash (CCFA), Ordinary Portland Cement (OPC) and Metakaolin (MK)

Raw Materials	CaO	SiO ₂	Al_2O_3	Fe ₂ O ₃	MgO	TiO ₂	K ₂ O	Na ₂ O	SO ₃	LOI (%)
CCFA	59.10	6.95	6.18	0.82	1.42	1.19	1.19	7.52	6.79	18.52
OPC	64.10	22.80	2.36	0.27	0.74	0.05	0.08	< 0.01	2.82	3.28
MK	0.33	55.83	44.03	1.86	0.29	< 0.01	0.42	0.51	0.35	0.54

LOI is loss of ignition at 1000 °C

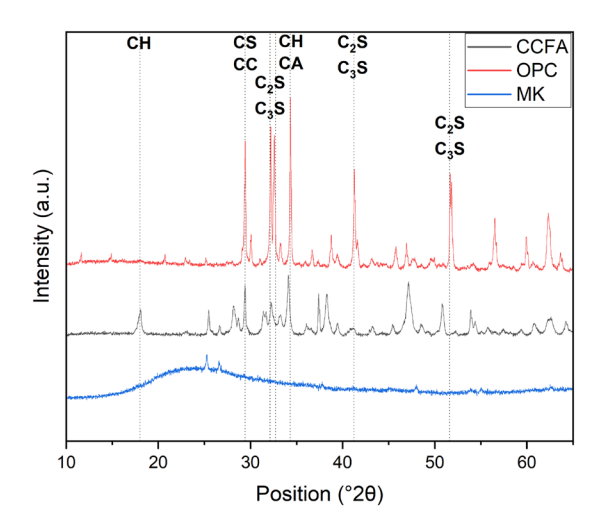


Fig. 1 XRD results of corrugated cardboard fly ash (CCFA), ordinary Portland cement (OPC) and metakaolin (MK). CC = calcite, CH = portlandite, $C_2S = dicalcium silicates$, $C_3S = tricalcium silicates$, CA = calcium aluminates

excess SO_3 content, loss on ignition over 7%, as well as being below the minimum compositional content of SiO_2 , Al_2O_3 , and Fe_2O_3 .

X-Ray Diffraction (XRD) Analysis

X-ray diffraction (XRD) analysis was conducted to examine the crystalline phases present in the CCFA using a PANalytical X'pert Powder X-ray diffractometer with Cu K_{α} radiation ($\lambda=1.51054$ Å) with generator settings of 45 kV, 40 mA. Data were collected in the range of 10–140° 2θ , with a step size of 0.013° 2θ and a measuring time of 89 s/step. The samples were rotated at 60 rpm during the data collection. The phases present were identified using the search-match function in HighScore Plus against the Crystallography Open Database.

Figure 1 shows that the OPC sample exhibits sharp peaks corresponding to crystalline phases such as trical-cium silicate (C_3S) and dicalcium silicate (C_2S), indicating a high degree of crystallinity. The CCFA sample displays a similar but less intense pattern, suggesting lower overall crystallinity. Notably, while calcium silicates (C_3S and

Table 2 Description of raw materials: D_{50} is the particle size distribution median (μ m), SSA = Specific surface area (m²/g), SD = density (g/cm³), MW = water content (%). D_{50} was taken from the particle size distribution, SSA from the BET analysis and SD and MW from laboratory testing

Raw Materials	D ₅₀	SSA	SD	MW
CCFA	16.65	4.4 ± 0.01	0.86	1.67
OPC	12.17	2.3 ± 0.02	1.40	0.38
MK	5.13	15.7 ± 0.08	0.44	0.50

 C_2S) are detectable in OPC, there is little to no indication of these in CCFA at approximately 33°, 42°, and 52°. Instead the dominant crystalline phase is calcium oxide (CaO).

This reduction in calcium silicate phases, coupled with an excess of free CaO, is expected to lead to the formation of excess calcium hydroxide (Ca(OH)₂) upon hydration. In the absence of reactive pozzolanic materials, this may negatively impact compressive strength. However, when sufficient pozzolans are present, the surplus Ca(OH)₂ can participate in secondary pozzolanic reactions, forming additional calcium silicate hydrate (C–S–H) and calcium aluminate silicate hydrate (C–A–S–H) gels that enhance mechanical performance.

The MK sample displays a broad hump, characteristic of an amorphous powder, indicating a predominantly non-crystalline structure.

Physical Properties and Particle Size Distributions

The physical properties of CCFA, OPC, and MK are presented in Table 2. Their particle size distributions, measured using a Malvern Mastersizer 3000, are shown in Fig. 2. CCFA had the largest median particle size $(D_{50} = 16.65 \,\mu\text{m})$ and exhibited the broadest particle size distribution. Interestingly, despite its larger particle size, CCFA demonstrated a higher specific surface area (4.4 m²/g) compared to OPC (2.3 m²/g), likely due to its inherent porosity, which could positively influence its reactivity.



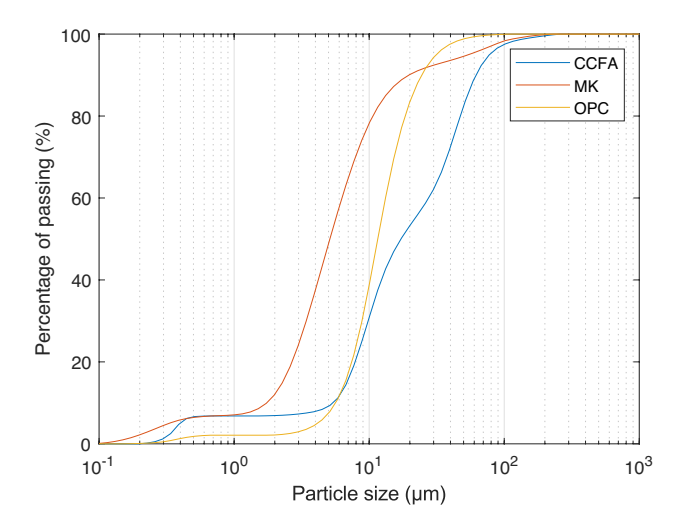


Fig. 2 Particle size distributions of corrugated cardboard fly ash (CCFA), ordinary Portland cement (OPC) and metakaolin (MK)

In contrast, MK had the smallest median particle size $(D_{50} = 5.13 \,\mu\text{m})$, the narrowest distribution, and notably the highest specific surface area (15.7 m²/g), factors known to significantly enhance its reactivity.

BET Analysis

Nitrogen adsorption–desorption isotherms at -196° C were collected with a Micromeritics ASAP2020 surface area analyser. Samples were degassed under vacuum at 300°C overnight prior to analysis. Surface areas were determined by the Brunauer-Emmett-Teller (BET) method, and Barrett-Joyner-Halenda (BJH) analysis was performed to determine pore-size distributions using the adsorption branch of the isotherms. Micropore surface areas were determined using t-plot analysis, while total pore volumes were calculated from the volume adsorbed at p/p_0 of 0.995.

The adsorption isotherms of OPC, MK, and CCFA were similar in shape and consistent with type IIb isotherms, typical of non-porous solids (Fig. 3a) [27]. The isotherms were not reversible, and a type H3 hysteresis loop with no

plateau at high relative pressures was observed in all three samples [28]. The area of the hysteresis loop increased in the order OPC < CCFA < MK, in agreement with the BJH pore-size distributions (Fig. 3b) and the specific surface areas (Table 1). The total pore volume of the three samples changed from $0.01~\rm cm^3~g^{-1}$ (OPC) and $0.02~\rm cm^3~g^{-1}$ (CCFA) to $0.10~\rm cm^3~g^{-1}$ (MK).

These results indicate that CCFA, with a greater pore volume than OPC, may contribute to increased early porosity and water uptake in mortars, which could reduce compressive strength due to calcium hydroxide formation, unless reactive additives are present [29, 30]. In contrast, MK's high surface area and porosity promote the development of C–S–H and C–A–S–H phases, improving densification and which could compensate for CCFA's limitations when used together.

Critique and Summary

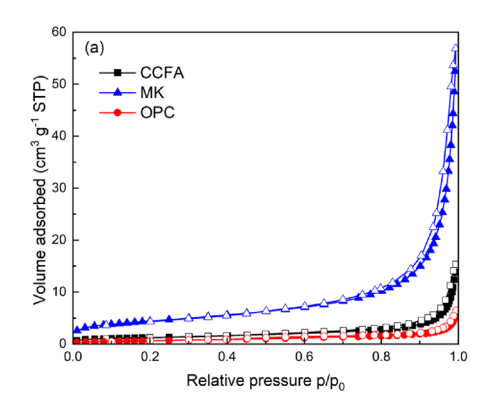
Comparison Between CCFA and Lime

The chemical composition of CCFA is notably different from that of traditional pozzolanic SCMs such as coal-derived fly ash and MK. While some SCMs are added for the pozzolanic activity due to being rich in silica (SiO₂) and alumina (Al₂O₃), instead CCFA is predominantly composed of calcium oxide (CaO), positioning it closer to lime as shown in the ternary diagram (Fig. 4). As Lime has no pozzolanic activity due to no silica and alumina content, the same will apply to CCFA with no, or little, pozzolanic activity expected. This fundamental difference distinguishes CCFA from coal derived fly ash or other SCMs traditionally used in concrete.

Why Metakaolin?

The XRD analysis of CCFA (Fig. 1) indicates that, although minor calcium silicates are present, the material is primarily composed of quicklime (CaO). Quicklime rapidly hydrates to form calcium hydroxide (Ca(OH)₂), supplying calcium

Fig. 3 a Nitrogen adsorption—desorption isotherms of CCFA, MK and OPC samples (solid symbols, adsorption; open symbols, desorption) and b corresponding adsorption BJH pore-size distributions



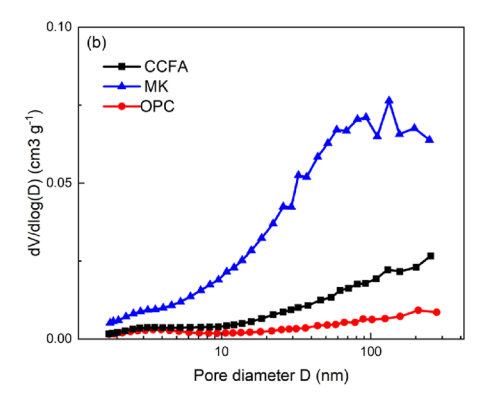
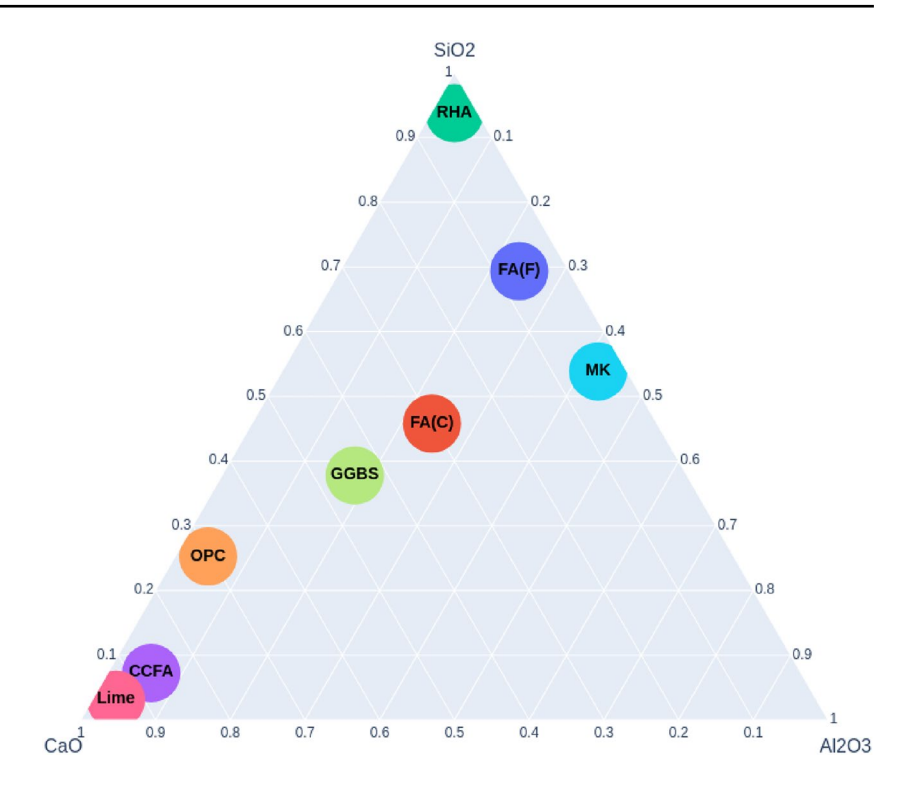




Fig. 4 Ca–Si–Al ternary diagram showing the chemical composition of various materials: FA(C)—Class C fly ash (high calcium content), FA(F)—Class F fly ash (low calcium, high silica content), RHA—Rice husk ash (high silica content), MK—Metakaolin, GGBS—Ground Granulated Blast Slag, Lime—Calcium oxide (CaO), OPC—Ordinary Portland cement, and CCFA—Corrugated cardboard fly ash



for potential strength development. However, CCFA lacks sufficient silica (SiO_2) and alumina (Al_2O_3), which are essential to produce the cementitious phases—calcium-silicate hydrate (C-S-H) and calcium-aluminosilicate hydrate (C-(A-)S-H)—that provide strength and durability in hydraulic cement systems.

Historically, quicklime has been used in lime-based mortars, which primarily harden through carbonation, a slow reaction in which Ca(OH)₂ interacts with atmospheric CO₂ to form calcium carbonate (CaCO₃) [31, 32]. While this process imparts long-term durability, it limits early strength development, posing challenges for modern construction applications.

To overcome these limitations, incorporating pozzolanic materials can enhance hydraulic properties, enabling faster strength development and improved durability [33–36]. Among pozzolans, metakaolin (MK) has garnered attention for its high reactivity and sustainability [37, 38]. Derived from the calcination of kaolin clay at temperatures of 600–900 °C, MK is composed primarily of aluminosilicates (50–55% SiO₂ and 40–45% Al₂O₃) [39, 40]. In the presence of calcium hydroxide, MK reacts to form C–S–H and C–(A–)S–H gels, enhancing the mechanical performance and durability of cementitious systems [31, 41–43].

Blending CCFA with MK capitalises on their complementary properties: CCFA's high CaO content provides a source of calcium, while MK supplies the aluminosilicates necessary to form strength-enhancing cementitious phases.

This synergy not only addresses the limitations of CCFA but also offers a novel pathway for sustainable concrete production using industrial by-products.

From a chemical perspective, the high calcium oxide content in CCFA hydrates to form calcium hydroxide, which subsequently reacts with the amorphous aluminosilicates (SiO₂ and Al₂O₃) present in MK. This pozzolanic reaction leads to the formation of calcium silicate hydrate (C–S–H), calcium aluminate hydrate (C–A–H), and calcium aluminosilicate hydrate (C–A–S–H) phases. The key reactions are summarised as follows [44, 45]:

$$Al_2O_3 \cdot 2SiO_2 + xCa(OH)_2 + H_2O$$

 $\rightarrow C-S-H + C-A-S-H + C_2ASH_8 + C_4AH_{13}$ (1)

The formation of these phases is crucial for improving the compressive strength, microstructural refinement, and durability of the hardened matrix. C–S–H acts as the principal strength-giving phase. The secondary aluminate hydrates–C₂ASH₈ and C₄AH₁₃—contribute to early strength and may undergo phase transformations over time, depending on the MK/CH ratio and curing conditions. Notably, the formation of C–A–S–H, particularly in systems with adequate Ca and Al availability, has been shown to enhance pore blocking and densify the matrix, leading to improved durability and reduced permeability [46].



Experimental Investigation of Compressive Strength of Mortar

This section illustrates the mix design, sample preparation and testing to study the effect of CCFA, MK and water-cement ratio (W/C) on mortar samples.

Design of Control Mortar Mix

The control mix was designed to achieve a target compressive strength of 30 MPa at 28 days, in accordance with BS EN 196-1 [47]. The mix was prepared using a cement-to-aggregate ratio of 1:3 by mass, with a water-to-cement ratio (W/C) of 0.55 to ensure sufficient workability during mixing and casting. The control mix serves as the baseline for evaluating the effects of incorporating CCFA and MK as partial cement replacements on compressive strength performance.

Test Samples Mix Design and Statistical Validations

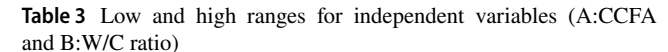
In this study, an I-optimal response surface methodology (RSM) was employed to systematically explore the influence of key factors on the performance of the mortar incorporating CCFA as a cement substitute. RSM uses statistical techniques to model and predict responses of interest to different input variables. I-optimality attempts to minimise the prediction variance over the design space to allow more accurate predictions with the resulting model, which evaluates linear and quadratic terms.

This approach was selected specifically to support post-experimental prediction of compressive strength across a broad range of mix designs. I-optimality was favoured over other design types (e.g., D-optimal or central composite) because it improves model prediction accuracy across the entire design space, rather than just enhancing parameter estimation [48]. This makes it particularly suitable for use cases where the fitted model will be used to formulate mixes of a known compressive strength.

A total of 16 experimental data points were required for this study, utilising an I-optimal experimental design that replicates points in the design space (Fig. 5) to minimise variance, and considering two independent variables. Each mix was replicated three times, and the resulting average compressive strength was used as the response variable. The response was analysed using the second-order polynomial equation:

$$y = f + aA + bB + cAB + dA^2 + eB^2$$
 (2)

where y is the response (compressive strength in this study), f is the intercept, A and B (see Tables 3 and 4 are the independent variables, a and b are the associated linear



Independent Variables	Unit	Variable Range		
		Low	High	
A: CCFA	%	0.0	40	
B: W/C ratio		0.45	0.7	

coefficients, c is the coefficient for the interaction between the variables, and d and e are the quadratic coefficients.

Statistical Analysis and Model Evaluation

The statistical analysis of the experimental data was conducted using Design-Expert® software (Stat-Ease Inc.). For each fitted model, several key indicators were used to assess statistical significance and predictive accuracy:

- F-value: The F-statistic evaluates the ratio of model variance to residual variance. A higher F-value indicates that the model explains a significant portion of the variability in the response compared to random error.
- *p-value*: The *p*-value represents the probability that the observed F-value could occur by chance. A *p*-value less than 0.05 indicates statistical significance, meaning the corresponding model term has a meaningful effect on the response variable.
- R²: The coefficient of determination quantifies how well the model fits the observed data. An R² value closer to 1.0 indicates a stronger fit.
- Adjusted R²: Adjusted R² accounts for the number of predictors in the model, providing a more accurate measure of goodness-of-fit for models with multiple terms.
- *Predicted R*²: This metric estimates how well the model is expected to predict responses for new observations.
- Lack-of-fit: This test evaluates the adequacy of the fitted model by comparing the variation not explained by the model to the pure error. A non-significant lack-of-fit (p-value ≥ 0.05) indicates that the model adequately describes the data without significant missing terms.

These statistical metrics are reported in the results and ANOVA sections to demonstrate the reliability and prediction accuracy of the fitted response surface models. The interaction terms (between CCFA and MK or W/C ratio) are also statistically evaluated based on their F-values and associated *p*-values.

To systematically evaluate the influence of different variables, the study was structured into two distinct experimental phases. The first phase explored the effect of CCFA as a percentage replacement of cement and variations in the



Fig. 5 Test samples mix design: a varying independent parameters are A: CCFA as a partial replacement of cement and B: W/C ratio, and b varying independent parameters are A: CCFA and B: MK as the partial replacement of cement. The numbers indicate replicated points in the design space. Those with no number were tested once

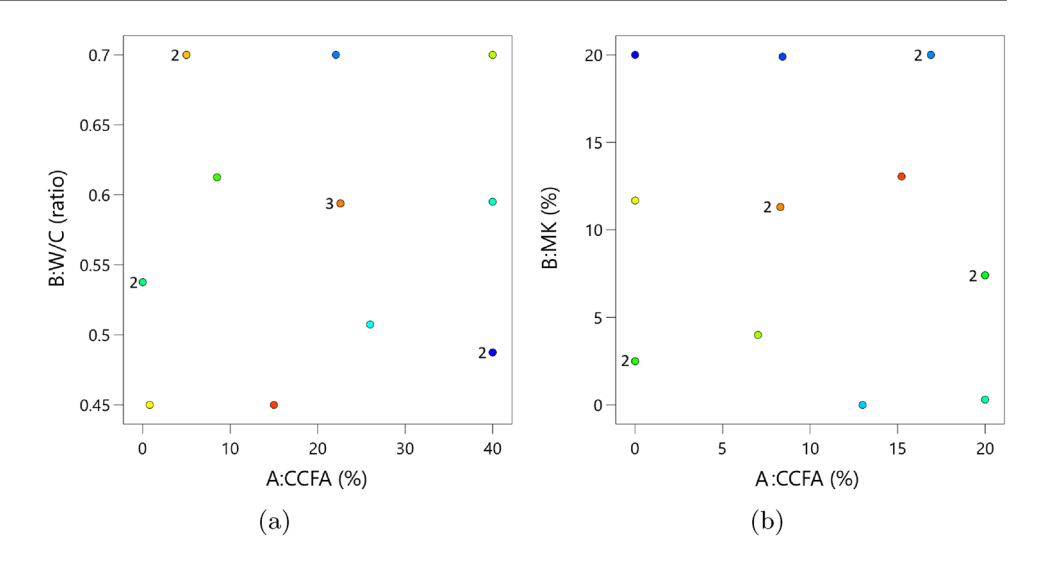


Table 4 Low and high ranges for independent variables (A:CCFA and B:MK)

Independent	Unit	Variable Range			
Variables		Low	High		
A: CCFA	%	0	20		
B: MK	%	0	20		

water-to-cement (W/C) ratio. The second phase investigated the combined effects of CCFA and MK as partial cement replacements, enabling assessment of potential synergy between a calcium-oxide rich waste product and a reactive pozzolan.

CCFA as Cement Replacement with W/C Ratio

Previous studies have shown that incorporating fly ash can reduce the water demand in mortar and concrete mixes [49–51], whereas ash from circulating fluidised bed combustion (CFBC) tends to increase water demand due to its high specific surface area and CaO content [50, 52]. Similarly, Dvorkin et al. [53] found that lime kiln dust, with a CaO content of 69%, significantly increases the water required for full hydration. Given that CCFA contains notable amounts of free lime (CaO), it is expected to similarly influence the water demand in cementitious mixes.

The W/C ratio experiment was, therefore, necessary to evaluate how CCFA influences both water requirements and the subsequent performance of mortar. Preliminary testing was conducted to identify an appropriate range of W/C ratios that would ensure workability across all mixes while also capturing performance trends, particularly compressive strength. The selected range of 0.45 to 0.70 allows for the assessment of CCFA's impact on hydration and strength development

under varying water contents, providing insights into its suitability for use in sustainable mortar systems.

This range was established based on initial mixing and workability observations rather than formal slump testing. Mixes with W/C ratios below 0.45 became too stiff and unworkable, while those exceeding 0.70 were overly fluid and unstable. The broad range was necessary due to the high free lime content in CCFA, which increases water demand during early hydration. Including this variable ensured that the experimental design captured the full range of realistic performance scenarios.

Table 3 summarises the independent variables: A, representing the CCFA percentage used to replace cement, and B, representing the water-to-cement (W/C) ratio. The table includes the low and high values for both variables. Figure 5a illustrates the test samples with varying percentages of A: CCFA and different ratios of B: W/C. The detailed mix designs for these samples are provided in Table 9 in Appendix A.

CCFA and Metakaolin as a Cement Replacement

As CCFA consists of non-pozzolanic components, which inherently lack hydration components [54]. Therefore, the addition of MK to the CCFA mortar was investigated. MK is well documented to allow air lime to exhibit hydration reactions, leading to increased strength and durability [55], due to the high CaO content of CCFA. Therefore, to assess the pozzolanic action of CCFA in the presence of MK, a further experiment was completed using the same I-optimal RSM.

The two input variables were defined as A: CCFA as a cement replacement and B: MK as a cement replacement, with the total binder content constant across all mixes. The ranges for these variables, outlined in Table 4, were chosen



to ensure that the maximum total cement replacement remained consistent, enabling direct comparison between mixes. The table includes the low and high values for both variables. Figure 5b illustrates the test samples with varying percentages of A: CCFA and B: MK. The detailed mix designs for these samples are provided in Table 10 in Appendix A.

Mortar Mix Preparation and Testing

All mortar samples were prepared following a consistent methodology. The binder materials (OPC, CCFA, and/or MK) were dry-mixed with fine aggregate at a fixed binder-to-aggregate ratio of 1:3 by mass. Water was then gradually added to achieve the desired water-to-cement (W/C) ratio as specified in each mix design. Mixing was performed using an automatic laboratory mortar mixer (Matest E093) to ensure homogeneity and workability. This procedure was used for all mixes prior to subsequent testing.

The synthesis of the mortar involved a series of standardized procedures to ensure consistent and reliable results. Firstly, cubic specimens with dimensions of 100 x 100 x 100 mm were prepared for compressive strength testing in accordance with BS EN 196-1 [47]. All mortar samples were prepared following a consistent methodology. The binder materials (OPC, CCFA, and/or MK) were dry-mixed with fine aggregate at a fixed binder-to-aggregate ratio of 1:3 by mass. Water was then gradually added to achieve the desired water-to-cement (W/C) ratio as specified in each mix design. Mixing was performed using an automatic laboratory mortar mixer (Matest E093) to ensure homogeneity and workability. This procedure was used for all mixes prior to subsequent testing. Once the mixing was complete, the mortar was allowed to set for 24 h under standard conditions of 20 ± 0.5 °C, promoting the initial hydration process. After the initial set, the specimens were carefully demoulded to maintain their shape and surface integrity.

To facilitate curing, the demoulded mortar specimens were submerged in water. This immersion in water provided a controlled and moist environment essential for appropriate hydration and development of strength. The curing process was carried out under standard conditions, maintaining a temperature of 20 ± 0.5 °C for 7 days and 28 days.

The compressive strength tests were performed using a universal testing machine in accordance with BS En 1015-11. Each specimen was placed between the upper and lower compression platens of the machine, ensuring proper alignment and even distribution of the load. A continuous compressive load was applied to the specimen at a controlled rate, until failure occurred. The loading rate was 50 N/s.



While mortar testing provides data on mechanical performance such as compressive strength, it includes fine aggregates that can obscure microstructural and chemical analyses. To isolate the behaviour of the binder system and better understand hydration mechanisms, phase development, and porosity, paste samples, composed solely of the binder components, were prepared. These paste specimens enable more accurate characterisation techniques such as XRD and BETRounded analysis.

Paste Casting and Curing Protocol

Paste mixes (binder only; no aggregates) were prepared according to the proportions listed in Table 5. Fresh pastes were cast into slabs and hydrated for 7 and 28 days under the same controlled conditions as the mortar specimens (Sect. 2). After curing, specimens were sectioned for subsequent characterisation as specified below.

X-Ray Diffraction on Hydrated Pastes

For XRD, paste slices of 5 mm thickness were analysed using a PANalytical X'pert Powder diffractometer with Cu K_{α} radiation (λ = 1.51054 Å) operated at 45 kV and 40 mA. Data were collected from 10–65° in 2 θ , step size 0.0167°, and 30 s/step. The in-situ hydrating samples were rotated at 60 rpm during the data collection. Phase identification employed HighScore Plus (search–match) with the Crystallography Open Database.

Nitrogen Adsorption (BET) on Hydrated Pastes

For BET analysis, cured paste of 2 cm thickness were prepared and hydrated for 28 days. Nitrogen adsorption—desorption isotherms were collected and analysed consistently with the procedure described in Sect. 2 (BET on raw materials), including determination of S_{BET}, BJH pore-size distributions from the adsorption branch, and t-plot micropore

Table 5 Mortar paste mix proportions for XRD and BET

Sample	OPC (%)	CCFA (%)	MK (%)
O100	100	0	0
O80-C20	80	20	0
O80-M20	80	0	20
O80-C10-M10	80	10	10
O60-C20-M20	60	20	20



areas where applicable. Total pore volume was calculated from the amount adsorbed at $p/p_0 = 0.995$.

Mechanical Characterisation of Hardened Mortars

Effect of CCFA % of Cement Replacement and W/C Ratio on Compressive Strength of Mortar

This section presents the results of an experimental investigation using MK and CCFA, as discussed in Sect. 3.2.2. As shown in Table 6, variable A is CCFA as a percentage of cement replacement, and variable B is W/C ratio. The fitted quadratic model for compressive strength at 7 days was statistically significant, with an R^2 of 96.56%, an adjusted R^2 of 94.39%, a predicted R^2 of 89.65%, and a lack of fit of 0.5695, described by Equation (3). Similarly, the fitted quadratic model for 28-day compressive strength was statistically significant, with an R^2 of 98.68%, an adjusted R^2 of 98.02%, a predicted R^2 of 97.11%, and a lack of fit of 0.1892, as shown in Equation (4).

$$f_{c,\text{wc7}} = 48.6 - 0.68A - 67.1B + 0.50AB + 0.0026A^2 + 26.4B^2$$
(3)

$$f_{c,\text{wc28}} = 74.0 - 12.9A - 96.1B + 1.02AB + 0.0085A^2 + 21.6B^2$$
 (4)

Where f_c is the maximum predicted compressive strength, A = %CCFA, and B = W/C ratio.

Figure 6 shows contour plots and 3D response surface plots for the compressive strength of mortars at 7 days and 28 days. As the developed models are significant, this allows a direct comparison between the two models. For all mixes, the compressive strength was lower for the 7-day samples,

Table 6 Analysis of variance (ANOVA) for compressive strength at 7 and 28 days for the mortar test samples varied with the percentage of CCFA and W/C ratio

Source	Compressi	ive Strength	Compressive Strength 28 Days		
	7 Days				
	F-Value	<i>p</i> -value	F-Value	<i>p</i> -value	
Model	51.5	< 0.0001	149	< 0.0001	
A-(%CCFA)	182	< 0.0001	374	< 0.0001	
B-(W/C)	49.4	< 0.0001	233	< 0.0001	
AB	4.08	0.0711	22.7	0.0008	
A^2	1.95	0.1923	27.1	0.0004	
\mathbf{B}^2	0.30	0.5978	0.26	0.6219	
Lack of Fit	0.088	0.5558	2.31	0.1892	

indicating that some hardening reactions during hydration occur after the initial 7-day period. The highest compressive strengths of the model occur at the lowest W/C ratio and the lowest CCFA percentage replacement. Conversely, the lowest compressive strength occurs at higher CCFA replacement and W/C ratio. As discussed previously, the inverse relationship between W/C and compressive strength is well documented [56, 57]. The inverse relationship between CCFA and compressive strength shows that the CCFA provided less compressive strength than OPC cement at all W/C ratios. The percentage gain in compressive strength between day 7 and day 28 was higher for mixes with greater CCFA replacements. Specifically, a mix containing 40% CCFA at a W/C ratio of 0.4875 exhibited a 58.3% increase in compressive strength from 7 to 28 days. In contrast, a mix with only 0.8% CCFA at a W/C ratio of 0.45 showed a 10.6% strength gain over the same period. At a fixed W/C ratio of 0.45, the response surface model predicted a 28-day compressive strength of 35.2 MPa for a mix with no CCFA, compared to 15.4 MPa for a mix with 40% CCFA replacement-corresponding to a 54.9% reduction in strength. This effect is likely due to a reduction in pozzolanic materials available in the paste with cement replacement, slowing down the hardening process of the mortar—this effect will be less notable at higher W/C due to the reduction of cementitious material per unit volume.

One contributing factor is the increased porosity introduced by CCFA-rich mixes. The high calcium oxide content in CCFA, coupled with limited pozzolanic reactivity, can result in an abundance of unreacted lime and a less dense hydration matrix (at higher W/C ratios). This increased porosity can negatively affect compressive strength, particularly at early ages. This is explored further through BET analysis of hardened pastes in Sect.5.2

Effect of Percentages of MK and CCFA on Compressive Strength of Mortar

This section presents the results of an experimental investigation using MK and CCFA, as discussed in Sect.3.2.3. As shown in Table 7, variable A is CCFA as a percentage cement replacement and variable B is MK as a percentage cement replacement. The fitted quadratic model for compressive strength at 7 days was statistically significant, with an R^2 of 96.57%, an adjusted R^2 of 94.67%, a predicted R^2 of 88.61%, and a lack of fit of 0.0171. This is described by Equation (5). Similarly, the fitted quadratic model of compressive strength at 28 days of curing age was statistically significant with an R^2 of 90.60%, an adjusted R^2 of 85.91%, a predicted R^2 of 72.71%, and a lack of fit of 0.4245. This is described by Equation (6).



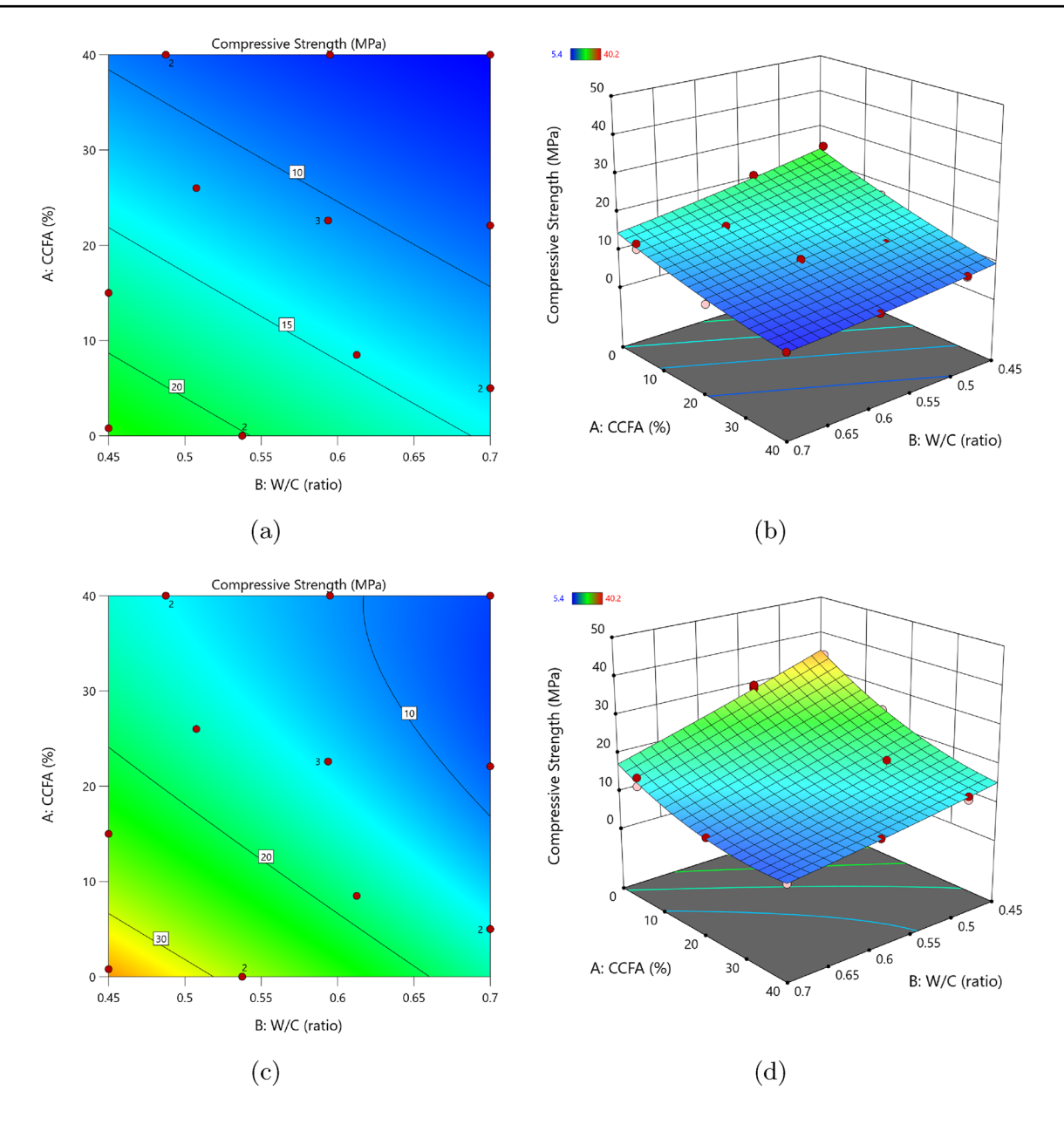


Fig. 6 The compressive strength is shown for both 7-day and 28-day samples using 2D contour plots (\mathbf{a}, \mathbf{c}) and 3D response surface plots (\mathbf{b}, \mathbf{d}) , illustrating its variation with the W/C ratio and percentage CCFA

$$f_{c,\text{mk7}} = 28.5 + 0.23A - 1.30B + 0.040AB + 0.0068A^2 + 0.029B^2$$
(5)

$$f_{c,\text{mk28}} = 35.1 + 0.036A - 1.10B + 0.034AB + 0.0092A^2 + 0.0186B^2$$
(6)

where f_c is the maximum predicted compressive strength, A = %MK, and B = %CCFA.

In this study, contour and surface plots of compressive strengths of mortar samples at 7 and 28 days to visualise the relationships between the key variables MK and CCFA (Fig. 7). These graphical representations offer valuable

insights into the effects of these variables on the response. However, it is important to note that while these visualisations provide a framework for understanding the trends and interactions, the lower adjusted and predicted R^2 values for the model suggest that there may be additional factors or intricacies influencing the compressive strength that are not fully accounted for in our model. While the response surface and contour plots offer valuable insights into the trends and interactions between variables, their interpretation must be viewed within the context of the model's assumptions and inherent limitations. The quadratic models used provide a strong statistical fit but may



Table 7 Analysis of variance (ANOVA) for varying percentages of MK and CCFA compressive strength at 7 and 28 days

Source	Compressi	ve Strength	Compressive Strength 28 Days		
	7 Days				
	F-Value	<i>p</i> -value	F-Value	<i>p</i> -value	
Model	50.7	< 0.0001	19.3	< 0.0001	
B-(%MK)	116	< 0.0001	47.3	< 0.0001	
A-(%CCFA)	58.9	< 0.0001	25.6	0.0005	
AB	45.5	< 0.0001	10.4	0.0092	
\mathbf{B}^2	0.815	0.3902	0.499	0.4960	
A^2	14.9	0.0038	2.05	0.1827	
Lack of Fit	11.6	0.0171	1.20	0.4245	

not fully capture complex non-linear behaviors or longterm effects beyond the experimental range. Therefore, further experimental validation is recommended to confirm these findings and extend their applicability.

The percentage gain in compressive strength between day 7 and day 28 was generally higher for mixes with higher CCFA replacement and lower MK replacement. For instance, mixes with 13% CCFA and 0% MK exhibited a 49% strength gain. However, mixes containing both CCFA and MK showed relatively lower strength gains between days 7 and 28, particularly when the replacement percentages were similar. For example, Run 13 and Run 14, both with 8.3% CCFA and 11.3% MK, demonstrated compressive strength gains of 24% and 26%, respectively.

The results of CCFA-MK blended mortar showed statistical significance for the variables MK and the interactive relationship between CCFA and MK. The lowest compressive strength results were observed with the highest CCFA replacement and no MK replacement, aligning with the results reported in Sect. 4.1. This trend reaffirms that CCFA does not inherently contribute to the hydraulic hardening of mortar. When MK was introduced without the presence of CCFA, the resulting compressive strength increased, which agrees with previous research [58], underlining the beneficial impact of MK on enhancing mortar strength. When MK was introduced with CCFA at higher percentages, the compressive strength equalled or exceeded the compressive strength of cement and MK alone. This suggests a potential synergy between MK and CCFA, confirmed by the statistically significant interaction in Table 7.

This shows that the CaO in CCFA forms Ca(OH)₂ during hydration, though the hardening is hindered due to the lack of pozzolanic material in the paste. The addition of MK then increases the formation of C–S–H and C–A–S–H gels from the available Ca(OH)₂, as shown in previous work with lime-metakaolin mortars [31, 41, 59, 60], though post-curing XRD analysis is required to confirm this. Together, they

form a mortar that hardens faster than lime alone, which has promising implications for sustainable construction practices and the utilisation of industrial waste products in cementitious systems. As CCFA is currently disposed of in landfills, this could allow for partial replacement of cement, resulting in mortar with a lower associated carbon emission.

Although metakaolin was used as the pozzolan in this study, similar synergistic behaviour may be achievable with other reactive aluminosilicate materials, such as coal fly ash, ground granulated blast-furnace slag, silica fume, or natural pozzolans. Exploring CCFA—pozzolan blends beyond metakaolin could broaden the applicability of this approach, particularly in contexts where MK is less available or more costly. Furthermore, while CCFA is not a stand-alone hydraulic binder under ambient curing, hydrothermal treatment to form calcium silicate phases may offer a pathway to increase its independent utilisation [61, 62]. However, such processing is typically energy-intensive and falls outside the scope of this low-temperature, low-carbon study.

The potential of CCFA as a cement replacement should be tested at higher replacement percentages to assess its suitability for cement replacement further. Additional research is essential to assess the durability aspects of CCFA-MK mortar in contrast to conventional OPC. This entails examinations encompassing freeze-thaw resistance, susceptibility to sulfate attack, chloride penetration, and carbonation, as well as conducting supplementary evaluations pertaining to permeability, sorptivity, water absorption, and shrinkage properties.

The potential of CCFA to participate in carbonation-based hardening, particularly under semi-dry or dry curing conditions, presents a promising avenue for further research. While traditional lime mortars rely on carbonation reactions—where Ca(OH)₂ slowly reacts with atmospheric CO₂ to form CaCO₃—such reactions can be significantly enhanced under elevated CO₂ environments [63]. Studies have highlighted the mineralogical and textural changes induced by both natural and forced carbonation in lime-based mortars [64], and a comprehensive overview of carbonation mechanisms and kinetics in these systems has been provided by Rodriguez-Navarro et al. [65]. These insights suggest that CCFA, owing to its high CaO content, may similarly benefit from carbonation curing methods to enhance long-term performance.

The predictive equations derived in this study (Equations 3, 4, 5, and 6) are specific to the experimental ranges used for CCFA, MK, and W/C ratio. These models are intended to guide formulation within these bounds and may not reliably extrapolate to inputs outside the tested ranges. Future studies involving alternative materials, curing conditions, or mix designs may require recalibration or redevelopment of the response surface models.



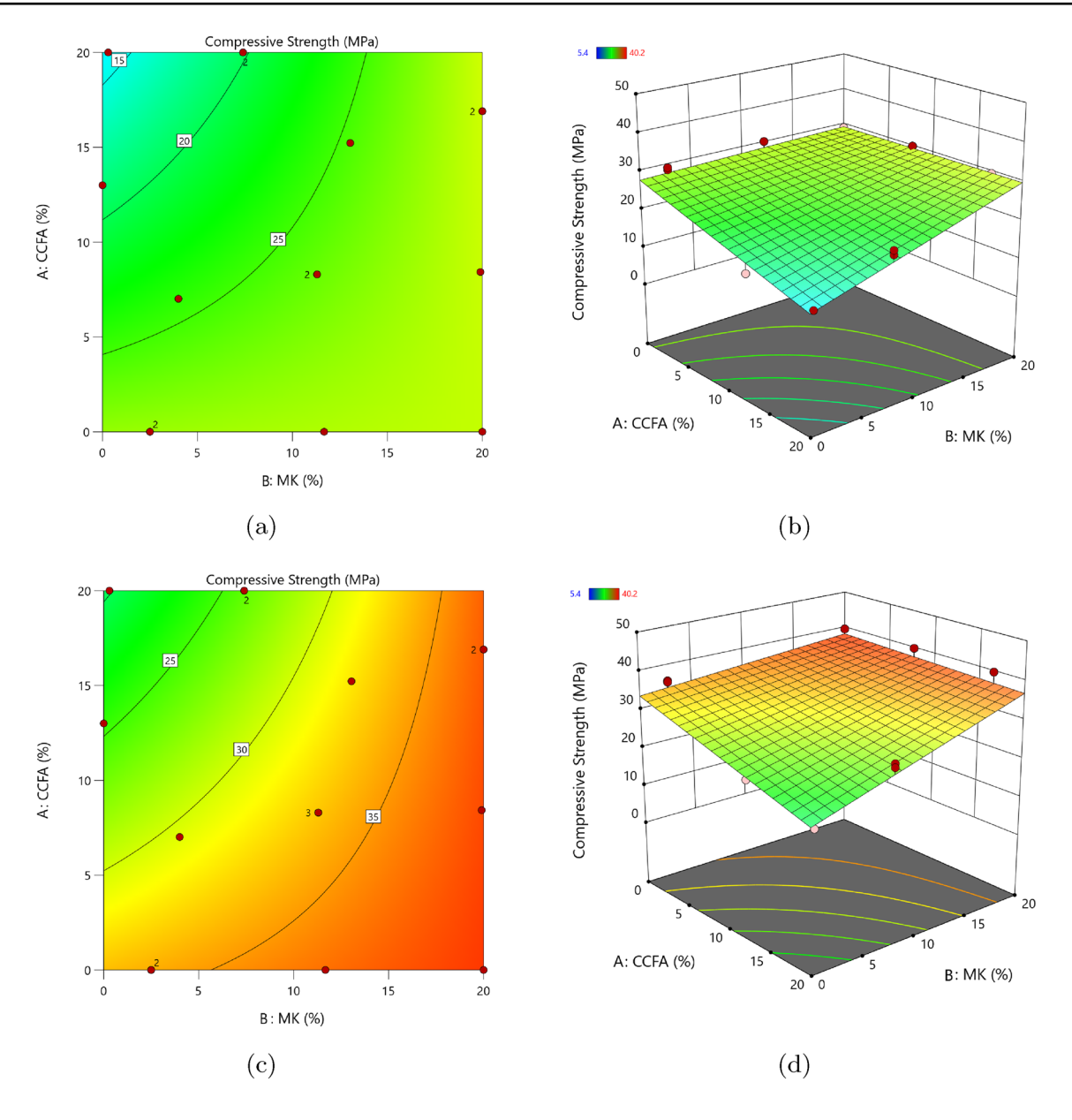


Fig. 7 The compressive strength is shown for both 7-day and 28-day samples using 2D contour plots (\mathbf{a}, \mathbf{c}) and 3D response surface plots (\mathbf{b}, \mathbf{d}) , illustrating its variation with the percentages CCFA and MK replacement

Characteristics of Hardened Binder Pastes

To complement the mechanical performance of the mortar mixes, the binder pastes (OPC, CCFA, MK in various proportions without aggregates) were examined using XRD at 7 and 28 days, and BET analysis at 28 days. These characterisation techniques reveal the evolution of hydration products and porous structure across the different binder systems, offering insight into the mechanisms responsible for strength development. Experimental procedures are detailed in Sect. 3.4.

X-Ray Diffraction

In the XRD analysis, calcium hydroxide peaks are observed in samples O100 and O80-C20. This peak is absent for the remaining samples, all of which contain MK, indicating that the MK is reacting with the excess calcium hydroxide (CH) in both CCFA and OPC which is consistent with the pozzolanic activity associated with MK-containing mixes. O100 and O80-C20 show limited change of calcium hydroxide between 7 and 28 days possibly due to limited access to pozzolanic materials. Ettringite formation is shown for all



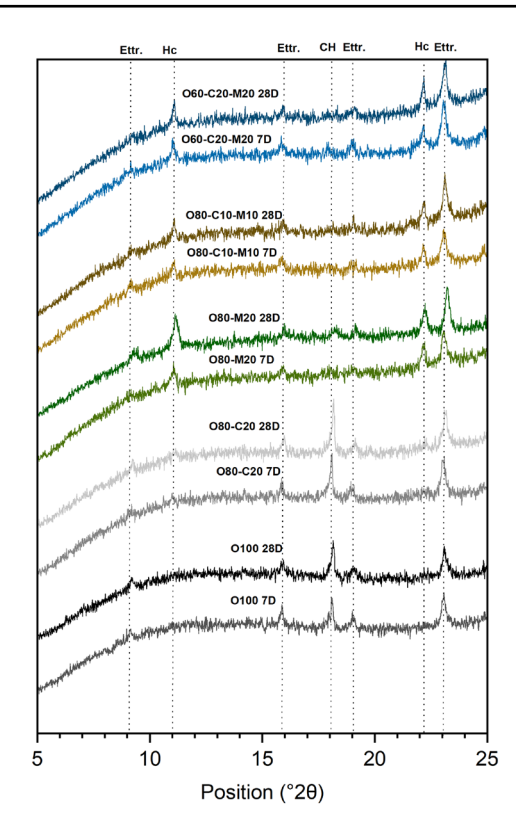


Fig. 8 XRD patterns for mortar paste hydrated for 7 days (7D) and 28 days (28D), where O = OPC, C = CCFA, and M = MK. Ettringite (Ettr.) formation is observed in all samples, while hemicarboaluminate (Hc) formation is present only in samples containing MK. A reduction in calcium hydroxide (CH) is evident in samples with MK

samples, and there seems to be little change between the 7-day and the 28-day samples.

The three samples containing MK show an increase in hemicarboaluminate (Hc) between 7 and 28 days. The samples containing only OPC and/or CCFA show no noticeable hemicarboaluminate formation, which is expected due to limited reactive alumina in these mixes (Fig. 8). This hemicarboaluminate phase, which previous studies on lime-blended cement have shown to reduce porosity, has been linked to improved compressive strength in resulting concrete [66–69].

BET Analysis

Upon 28-days hydration, the nitrogen adsorption isotherms for all 5 samples (Table 5) yielded type IIb isotherms with more pronounced type H3 hysteresis loops (Fig. 9a and c) compared to the raw materials (Fig. 3). The type H3 loop is typically observed with aggregates of plate-like particles giving rise to slit-shaped pores [28].

The surface areas (Table 8) of all hydrated samples increased compared to the surface areas of the raw materials (Table 2), with the largest increase observed for the O80-C20 sample. The higher surface area of the O80-C20 sample

Table 8 BET surface areas (S_{BET}) , micropore areas (S_{micro}) , and total pore volumes (V_{total}) of the 28 days-hydrated materials and mixtures

S_{BET} (m ² /g)	S _{micro} (m ² /g)	V _{total} (cm ³ /g)
47.5 ± 0.19	n.d	0.13
77.5 ± 0.40	n.d	0.17
63.5 ± 0.21	6.7	0.25
64.9 ± 0.15	1.8	0.18
57.9 ± 0.12	2.1	0.19
	47.5 ± 0.19 77.5 ± 0.40 63.5 ± 0.21 64.9 ± 0.15	47.5 ± 0.19 n.d 77.5 ± 0.40 n.d 63.5 ± 0.21 6.7 64.9 ± 0.15 1.8

Note: n.d. = not detected

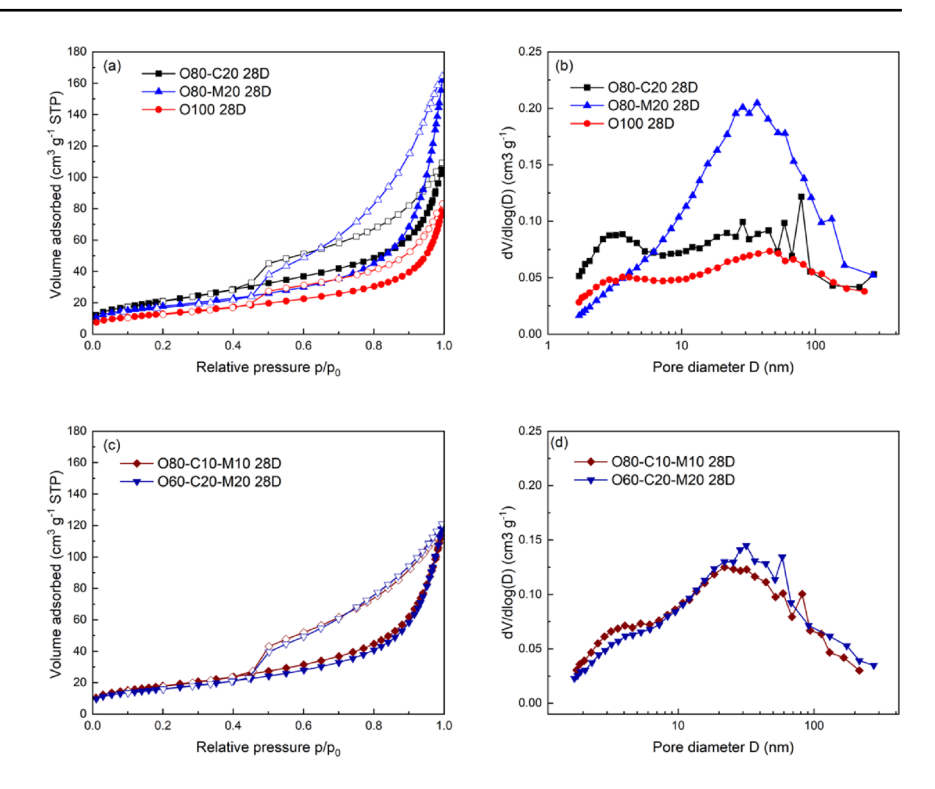
compared to the O80-M20 sample after hydration could be associated with the presence of hemicarboaluminate in the latter. The total pore volume followed O80-M20 > O80-C20 > O100, with microporosity observed specifically in the hydrated samples with MK, as shown in Table 8. Although total pore volumes and the mesopore-size distribution for samples with H3 type hysteresis loop cannot be assessed reliably [28], the total pore volumes in Table 8 and the poresize distribution provided in Fig. 9b and d can be used to provide a qualitative assessment of the porous structures of the hydrated samples. A peak between 1.5 and 5.5 nm was observed for all samples except O80-M20; its intensity decreased in the order $O80-C20 \gg O80-C10-M10 > O60-$ C20-M20 > O100. The shape of this peak changed for the O80-C10-M10 and O60-C20-M20 samples, particularly for the O60-C20-M20 sample, for which it resembled a shoulder rather than a peak. The changes are consistent with the composition of the mixed samples containing MK of increasing mass fraction from O80-C10-M10 to O60-C20-M20.

The broader peak between 6 and 200 nm for the mixed samples was between the hydrated O80-M20 and O80-C20 and O100 peaks (Fig. 9b and d). The surface areas and total pore volumes of the O80-C10-M10 and O60-C20-M20 samples also changed as expected based on the composition of these samples and the surface areas and pore volumes of the hydrated O100, O80-C20 and O80-M20, including the level of microporosity detected.

The results from the adsorption isotherm measurements and corresponding BJH pore-size distributions further confirm a combined chemical and physical synergy between CCFA and MK, allowing for mortar formulations with compressive strengths exceeding that of OPC alone. In this system, the CaO-rich but non-pozzolanic CCFA supplies calcium hydroxide, which reacts with the pozzolanic metakaolin to produce additional C–S–H and C–A–S–H gels. These secondary hydration products fill and refine existing pore spaces, leading to a denser microstructure and improved mechanical performance. The subtle differences in the pore structures of O80-C10-M10 and O60-C20-M20, mainly in the volume of gas adsorbed in pores smaller than 5.5 nm, suggest that the level of microporosity associated



Fig. 9 a, c Nitrogen adsorption—desorption isotherms of 28-days hydrated CCFA, MK and OPC samples (a) and 10% and 20% OPC-CCFA-MK mixtures (c) (solid symbols, adsorption; open symbols, desorption) and b, d corresponding adsorption BJH pore-size distributions



with MK reactivity contributes to the compressive strength of the blended mortars.

Although a pronounced mesopore peak near 30-50 nm was observed for the MK-containing samples at 28 days, this feature does not indicate weaker microstructures. For type H3 hysteresis loops, BJH analysis provides only a qualitative pore-size distribution. In pozzolanic systems such as those containing MK, coarser capillaries (>100 nm) are progressively refined into mesopores as secondary C-A-S-H gels form, increasing the overall gel/space ratio and reducing pore connectivity-both of which enhance strength. This interpretation is consistent with the observations of Zeng et al. [70], who reported that at 28 days fly-ash-blended pastes exhibited a temporary increase in 50-100 nm pores that diminished by 90 days as pozzolanic reactions continued. In our study, the MK-containing samples already show evidence of this refinement process at 28 days, explaining their higher compressive strength compared with the O80-C20 blend, where no pozzolan was added. The O80-C20 paste, dominated by unreacted Ca(OH)₂ and larger interconnected capillaries, retained the coarsest pore network and therefore the lowest strength. A distinct hump near 2 nm is also visible for O80-C20, corresponding to the characteristic pore feature of unreacted calcium hydroxide [71]. In contrast, the MK blends display reduced very-large-pore volume and a diminished ~2 nm gel-pore feature, reflecting a denser and more cohesive microstructure consistent with continuing pozzolanic activity.

Summary

The reduced compressive strength observed in CCFA-rich mixes is primarily attributed to increased matrix porosity and the limited pozzolanic reactivity of CCFA. XRD analysis supports this interpretation, revealing the presence of unreacted calcium hydroxide in the hardened samples.

The compressive strength results align closely with the microstructural and surface area findings, providing insight into the influence of CCFA and MK on mortar performance. BET analysis revealed that hydrated samples containing CCFA had a higher specific surface area compared to OPC alone, indicating increased porosity and the potential presence of unreacted CCFA particles. The lower compressive strength observed in CCFA-rich samples can be attributed to this increased porosity, as well as the limited pozzolanic reactivity of CCFA. XRD analysis further supports this, revealing residual calcium hydroxide in the hardened matrix. The increase in pore diameter volume between 1–5 nm observed in the O80-C20 sample corresponds with that of unreacted calcium hydroxide [71].

XRD analysis identified crystalline calcium hydroxide and ettringite as predominant phases in CCFA-rich samples, with reduced C–S–H and C–(A)–S–H formation compared to MK-containing samples. The incorporation of MK significantly improved the matrix densification due to its high pozzolanic reactivity, as evidenced by increased hydration product formation and the reduction of CH peaks in XRD patterns.



The trends in compressive strength mirror these observations. Samples with higher MK content exhibited greater compressive strength, correlating with denser hydration products and improved pore structure as indicated by BET and XRD analyses. Conversely, the CCFA-rich samples showed lower compressive strength due to the limited reactivity of CCFA and associated increase in porosity.

Overall, the integration of compressive strength, BET, and XRD analyses underscores the complementary roles of CCFA and MK in hydrated mortars. MK enhances the pozzolanic reaction, leading to improved phase development and microstructural integrity, while CCFA, without the added MK, contributes primarily as a filler material with limited hydraulic activity. These findings highlight the importance of balancing CCFA and MK content to optimise mortar performance.

Conclusion

This study investigated the influence of CCFA as a partial replacement for cement in mortar, focusing on its impact on compressive strength. CCFA was characterised using XRD, XRF, BET, and particle size analysis. Two distinct experiments were conducted using a response surface methodology to test compressive strength of mortar samples: the first with CCFA as a cement replacement and W/C ratio; and the second with CCFA as a cement replacement and MK as a cement replacement. Hardened mortar pastes were characterised using XRD and BET. The main conclusions are as follows:

- CCFA replacement of cement alone had a negative correlation with compressive strength when the mortar was cured in a high-humidity environment. In addition, an increase in the W/C ratio showed a reduction in compressive strength at all CCFA replacements.
- Comparing 7-day and 28-day compressive strengths showed that 90% of compressive strength was achieved after 7 days for the highest W/C ratio and lowest CCFA replacement; conversely, the lowest W/C ratio and highest CCFA replacement achieved 45% of the 28-day compressive strength in 7 days.
- 3. Blended mortars, when replacing OPC with 20% CCFA and 20% MK, resulted in compressive strengths equal to those achieved by cement and 20% MK when cured in a high-humidity environment. These significant results showed a synergy between MK and CCFA, providing an avenue for sustainable construction materials.
- 4. XRD analysis of hydrated mortar pastes revealed a reduction in calcium hydroxide in samples containing metakaolin, indicating enhanced pozzolanic activity. BET data suggest that the excess calcium hydroxide

- present in CCFA reacted to form strength-contributing phases such as C–S–H and C–(A)–S–H gels, improving the microstructural integrity of the mortar.
- 5. Comprehensive characterisation of CCFA revealed its high calcium oxide content and limited pozzolanic activity, distinguishing it from traditional fly ashes. XRD confirmed the dominance of quicklime and minor calcium silicate phases, while BET analysis indicated a higher specific surface area and porosity compared to OPC. These properties suggest that CCFA primarily acts as a filler material in a hydraulic setting, but with the potential to contribute to hydration through the reaction of calcium hydroxide, particularly when combined with a reactive pozzolan like metakaolin.

Despite the promising performance of CCFA-MK blends at the laboratory scale, several limitations and challenges must be addressed before large-scale industrial implementation. The variability in the chemical composition of CCFA, due to differences in feedstock and incineration conditions, poses a reproducibility risk that may affect mechanical performance. Additionally, the high sulphur content may result in durability concerns such as delayed ettringite formation or shrinkage unless carefully controlled. Further challenges include the logistics of sourcing consistent CCFA, adapting existing mixing protocols, and ensuring compliance with construction standards and regulatory frameworks. Future research should explore the long-term performance, life-cycle impact, and potential pre-treatment of CCFA to ensure safe and scalable use in commercial cementitious products.

This research benefits both the cardboard paper and concrete industries. In the cardboard industry, a significant challenge is the disposal of waste cardboard in landfills, which generates methane-a greenhouse gas far more potent than carbon dioxide. While recycling waste cardboard is the ideal solution, it is not always feasible. As an alternative, some companies opt for waste combustion to recover energy, converting the cardboard sludge into ash, which results in lower emissions when landfilled. However, this method introduces the challenge of managing fly ash disposal. Although fly ash produces minimal harmful emissions, it can contaminate soil and water with heavy metals. This study demonstrates that CCFA can be used as a partial substitute for cement, thereby reducing the concrete industry's carbon footprint. Simultaneously, it addresses the issue of fly ash disposal by converting waste into a valuable resource, creating a potential business opportunity.

Appendix A

See Tables 9 and 10.



Table 9 Mix proportions and corresponding compressive strengths at 7 and 28 days, showing the effect of CCFA replacement percentage and W/C ratio

Mix	CCFA (%)	W/C	CCFA (kg/m ³)	OPC (kg/m ³)	Water (kg/m ³)	Fine Aggregate (kg/m ³)	7-Day (MPa)	28-Day (MPa)
1	40.0	0.49	161.3	242.0	191.5	1209.8	8.53	13.26
2	22.6	0.59	89.7	307.1	235.6	1190.2	10.00	13.28
3	22.1	0.70	84.1	296.9	266.7	1143.1	7.17	9.13
4	40.0	0.49	160.5	240.7	195.6	1203.7	8.80	14.18
5	26.0	0.51	106.1	302.1	207.2	1224.7	11.96	18.43
6	40.0	0.60	153.9	230.8	228.9	1153.9	6.93	10.91
7	0.0	0.54	0.0	423.2	227.5	1269.6	20.89	29.64
8	5.0	0.70	19.6	372.9	274.7	1177.5	14.12	15.98
9	0.0	0.54	0.0	423.2	227.5	1269.6	17.56	28.72
10	8.5	0.61	34.3	369.6	247.4	1211.6	15.01	16.65
11	22.6	0.59	89.7	307.1	235.6	1190.2	11.72	13.18
12	40.0	0.70	147.9	221.8	258.8	1109.1	5.45	7.66
13	0.8	0.45	3.5	435.3	197.5	1316.4	24.83	34.12
14	5.0	0.70	19.6	372.9	274.7	1177.5	12.66	13.68
15	22.6	0.59	89.7	307.1	235.6	1190.2	11.48	12.77
16	15.0	0.45	64.0	362.8	192.1	1280.6	16.73	24.12

All values rounded to reflect the precision of the measurements and instrument limitations

Table 10 Mix proportions and corresponding compressive strengths at 7 and 28 days, showing the effect of MK and CCFA as partial cement replacements

Mix	MK (%)	CCFA (%)	MK (kg/m ³)	CCFA (kg/m ³)	OPC (kg/m ³)	Water (kg/m ³)	Fine Aggregate (kg/m³)	7-Day (MPa)	28-Day (MPa)
1	20.0	0.0	74.4	0.0	297.7	204.7	1116.5	29.19	39.70
2	19.9	8.4	73.1	30.9	263.2	202.0	1101.6	30.37	40.14
3	20.0	16.9	72.4	61.2	228.4	199.1	1085.8	29.74	39.95
4	0.0	13.0	0.0	53.4	357.5	226.0	1232.7	16.11	23.99
5	2.5	0.0	10.4	0.0	403.8	227.8	1242.6	28.87	36.02
6	0.3	20.0	1.2	81.0	322.7	222.7	1214.7	14.34	18.99
7	7.4	20.0	28.7	77.5	281.3	213.1	1162.6	21.48	28.66
8	7.4	20.0	28.7	77.5	281.3	213.1	1162.6	22.63	27.65
9	2.5	0.0	10.4	0.0	403.8	227.8	1242.6	29.43	35.68
10	20.0	16.9	72.4	61.2	228.4	199.1	1085.8	29.71	33.53
11	4.0	7.0	16.2	28.4	360.4	222.7	1215.0	22.55	29.82
12	11.7	0.0	45.6	0.0	345.4	215.1	1173.1	30.49	34.85
13	11.3	8.3	43.7	32.1	310.6	212.5	1158.9	25.20	31.22
14	11.3	8.3	43.7	32.1	310.6	212.5	1158.9	25.10	31.69
15	13.0	15.2	49.3	57.5	271.0	207.8	1133.4	23.16	31.10
16	11.3	8.3	43.7	32.1	310.6	212.5	1158.9	24.99	31.64

Fine aggregate masses were recalculated using the absolute volume method to account for differing densities of OPC, CCFA and MK. All values rounded to reflect measurement precision

Acknowledgements The authors would like to express their gratitude to Antony Burrage at the University of Salford for his invaluable assistance with compressive strength testing. Special thanks are also extended to Hayley Andrews and David McKendry for their support, which significantly contributed to the material characterisation in this study.

Author Contributions Silvia Tedesco and Aron Teklemariam contributed to the study conception and design. Levingshan Augusthus-Nelson provided overall guidance on the experimental approach and access to testing facilities. Material preparation, data collection and analysis were performed by Erik Christopher Hallsworth. The first draft of the manuscript was written by Erik Christopher Hallsworth and Lubomira



Tosheva, and revised with input from Levingshan Augusthus-Nelson, Aron Teklemariam, Sergio Davies and Silvia Tedesco. All authors commented on the submitted version of the manuscript. All authors read and approved the final manuscript.

Funding This research was funded by the Department of Engineering at Manchester Metropolitan University. The authors are grateful for the financial and institutional support, as well as the resources and facilities provided, which were essential to the successful completion of this project.

Data Availability All data generated or analysed during this study are included in this published article.

Declarations

Conflict of interest The authors have no relevant financial or non-financial interests to disclose.

Open Access This article is licensed under a Creative Commons Attribution 4.0 International License, which permits use, sharing, adaptation, distribution and reproduction in any medium or format, as long as you give appropriate credit to the original author(s) and the source, provide a link to the Creative Commons licence, and indicate if changes were made. The images or other third party material in this article are included in the article's Creative Commons licence, unless indicated otherwise in a credit line to the material. If material is not included in the article's Creative Commons licence and your intended use is not permitted by statutory regulation or exceeds the permitted use, you will need to obtain permission directly from the copyright holder. To view a copy of this licence, visit http://creativecommons.org/licenses/by/4.0/.

References

- GlobeNewswire, Corrugated Board Packaging Global Strategic Business Report, https://www.globenewswire.com/news-relea se/2024/12/17/2998150/28124/en/Corrugated-Board-Packa ging-Strategic-Business-Report-2024-Single-Wall-Board-Packa ging-Segment-is-Forecast-to-Reach-US-2-3-Billion-by-2030with-a-CAGR-of-a-3-9-Forecasts-to-2030.htmlglobenewswire. com report. Accessed 7 Jan. 2025 (2024)
- Larre, A.V., Wenzel, H.: Paper waste recycling, incineration or landfilling? Rev. Exist. Life Cycle Assessm. Waste Manag. 8, 13 (2007)
- UK Government, UK Statistics on Waste, https://www.gov. uk/government/statistics/uk-waste-data/uk-statistics-on-waste. Accessed 8 Jan. 2025 (2025)
- 4. Iyer, R.: The surface chemistry of leaching coal fly ash. J. Hazard. Mater. **93**(3), 321–329 (2002)
- Janoš, P., Wildnerová, M., Loučka, T.: Leaching of metals from fly ashes in the presence of complexing agents. Waste Manage. 22(7), 783–789 (2002)
- Cho, Y.K., Jung, S.H., Choi, Y.C.: Effects of chemical composition of fly ash on compressive strength of fly ash cement mortar. Constr. Build. Mater. 204, 255–264 (2019). https://doi.org/10.1016/j.conbuildmat.2019.01.208
- Herath, C., Gunasekara, C., Law, D.W., Setunge, S.: Performance of high volume fly ash concrete incorporating additives: a systematic literature review. Constr. Build. Mater. 258, 120606 (2020). https://doi.org/10.1016/j.conbuildmat.2020.120606
- Krithika, J., Ramesh Kumar, G.B.: Influence of fly ash on concrete: a systematic review. Mater. Today Proc. 33, 906–911 (2020). https://doi.org/10.1016/j.matpr.2020.06.425

- Liu, M., Wu, H., Yao, P., Wang, C., Ma, Z.: Microstructure and macro properties of sustainable alkali-activated fly ash mortar with various construction waste fines as binder replacement up to 100 https://doi.org/10.1016/j.cemconcomp.2022.104733
- Mavroulidou, M., Feruku, B., Boulouki, G.: Properties of structural concrete with high-strength cement mixes containing waste paper sludge ash. J. Mater. Cycles Waste Manage. 24(4), 1317–1332 (2022)
- Jwaida, Z., Dulaimi, A., Alyhya, W., Algretawee, H., Al-Busaltan, S.: Recycling and utilization of paper sludge ash-current status review and future perspectives. Sustain. Mater. Tech. 40 (2024)
- 12. Grist, E.R., Paine, K.A., Heath, A., Norman, J., Pinder, H.: The environmental credentials of hydraulic lime-pozzolan concretes. J. Clean. Prod. **93**, 26–37 (2015)
- Walker, R., Pavía, S.: Physical properties and reactivity of pozzolans, and their influence on the properties of lime-pozzolan pastes. Mater. Struct. 44, 1139–1150 (2011)
- Malathy, R., Shanmugam, R., Dhamotharan, D., Kamaraj, D., Prabakaran, M., Kim, J.: Lime based concrete and mortar enhanced with pozzolanic materials-state of art. Constr. Build. Mater. 390, 131415 (2023)
- Pavlík, V., Užáková, M.: Effect of curing conditions on the properties of lime, lime-metakaolin and lime-zeolite mortars. Constr. Build. Mater. 102, 14–25 (2016). https://doi.org/10.1016/j.conbuildmat.2015.10.137
- Gameiro, A., Santos Silva, A., Faria, P., Grilo, J., Branco, T., Veiga, R., Velosa, A.: Physical and chemical assessment of limemetakaolin mortars: influence of binder:aggregate ratio. Cem. Concr. Compos. 45, 264–271 (2014). https://doi.org/10.1016/j. cemconcomp.2013.10.006
- Grilo, J., Santos Silva, A., Faria, P., Gameiro, A., Veiga, R., Velosa, A.: Mechanical and mineralogical properties of natural hydraulic lime-metakaolin mortars in different curing conditions. Constr. Build. Mater. 51, 287–294 (2014). https://doi.org/ 10.1016/j.conbuildmat.2013.10.087
- Grist, E.R., Paine, K.A., Heath, A., Norman, J., Pinder, H.: Structural and durability properties of hydraulic lime-pozzolan concretes. Cement Concr. Compos. 62, 212–223 (2015). https://doi.org/10.1016/j.cemconcomp.2015.04.011
- Barbhuiya, S.A., Gbagbo, J.K., Russell, M.I., Basheer, P.A.M.: Properties of fly ash concrete modified with hydrated lime and silica fume. Constr. Build. Mater. 23(10), 3233–3239 (2009). https://doi.org/10.1016/j.conbuildmat.2009.06.002
- Krejsová, J., Koňáková, D., Pommer, V., Poláková, L., Ćerný, R., Maděra, J., Vejmelková, E.: Valorization of waste wood fly ash in environmentally friendly lime-based plasters with enhanced strengths for renovation purposes. J. Build. Eng. 87, 109056 (2024). https://doi.org/10.1016/j.jobe.2024.109056
- Li, L.G., Lin, Z.H., Chen, G.M., Kwan, A.K.H.: Reutilizing clay brick dust as paste substitution to produce environment-friendly durable mortar. J. Clean. Prod. 274, 122787 (2020). https://doi. org/10.1016/j.jclepro.2020.122787
- Su-Cadirci, T.B., Calabria-Holley, J., Ince, C., Ball, R.J.: Freezethaw resistance of pozzolanic hydrated lime mortars. Constr. Build. Mater. 394, 131993 (2023). https://doi.org/10.1016/j.conbu ildmat.2023.131993
- Li, Q., Qiao, H., Li, A., Li, G.: Performance of waste glass powder as a pozzolanic material in blended cement mortar. Constr. Build. Mater. 324, 126531 (2022). https://doi.org/10.1016/j.conbuildmat. 2022.126531
- Matos, A.M., Sousa-Coutinho, J.: Durability of mortar using waste glass powder as cement replacement. Constr. Build. Mater. 36, 205– 215 (2012). https://doi.org/10.1016/j.conbuildmat.2012.04.055
- BS EN 197-1: Cement Composition, Specifications, and Conformity Criteria for Common Cements. Accessed Jan. 2025 (2011)



- BS 8615-1: Pozzolanic Materials Specifications for Pulverised-Fuel Ash for Use with Portland Cement. Accessed Jan. 2025 (2019)
- 27. Rouquerol, F., Rouquerol, J., Sing, K.: Adsorption by Powders and Porous Solids. Academic Press, London (1999)
- Sing, K.S., Williams, R.T.: Physisorption hysteresis loops and the characterization of nanoporous materials. Adsorpt. Sci. Tech. 22(10), 773–782 (2004)
- Zhao, H., Xiao, Q., Huang, D., Zhang, S.: Influence of pore structure on compressive strength of cement mortar. Sci. World J. 2014(1), 247058 (2014)
- Lootens, D., Bentz, D.P.: On the relation of setting and early-age strength development to porosity and hydration in cement-based materials. Cement Concr. Compos. 68, 9–14 (2016)
- Pavlík, V., Užáková, M.: Effect of curing conditions on the properties of lime, lime-metakaolin and lime-zeolite mortars. Constr. Build. Mater. 102, 14–25 (2016). https://doi.org/10.1016/j.conbuildmat.2015.10.128
- 32. Cizer, K.V., Balen, D.V.: Gemert, Competition between hydration and carbonation in hydraulic lime and lime-pozzolana mortars. Adv. Mater. Res. **133**, 241–246 (2010)
- Bauerová, P., Reiterman, P., Pavlíková, M., Štorkánová, M.K., Keppert, M.: Fresh state properties of lime mortars with flax oil admixture. Acta Polytechnica CTU Proc. 22, 7–11 (2019)
- Papayianni, I., Stefanidou, M.: Strength–porosity relationships in lime–pozzolan mortars. Constr. Build. Mater. 20(9), 700–705 (2006)
- Vejmelková, E., Keppert, M., Keršner, Z., Rovnaníková, P., Černý,
 R.: Mechanical, fracture-mechanical, hydric, thermal, and durability properties of lime-metakaolin plasters for renovation of historical buildings. Constr. Build. Mater. 31, 22–28 (2012)
- Vejmelková, E., Keppert, M., Rovnaníková, P., Keršner, Z., Černý,
 R.: Application of burnt clay shale as pozzolan addition to lime mortar. Cement Concr. Compos. 34(4), 486–492 (2012)
- Gruber, K., Ramlochan, T., Boddy, A., Hooton, R., Thomas, M.: Increasing concrete durability with high-reactivity metakaolin. Cement Concr. Compos. 23(6), 479–484 (2001)
- Onyelowe, K., Naghizadeh, A., Aneke, F., Kontoni, D.-P., Onyia, M., Welman-Purchase, M., Ebid, A., Adah, E., Stephen, L.U.: Characterization of net-zero pozzolanic potential of thermallyderived metakaolin samples for sustainable carbon neutrality construction. Sci. Rep. 13(1), 18901 (2023)
- Poon, C.-S., Lam, L., Kou, S., Wong, Y.-L., Wong, R.: Rate of pozzolanic reaction of metakaolin in high-performance cement pastes. Cem. Concr. Res. 31(9), 1301–1306 (2001)
- Rashad, A.M.: Metakaolin as cementitious material: history, scours, production and composition – a comprehensive overview. Constr. Build. Mater. 41, 303–318 (2013). https://doi.org/ 10.1016/j.conbuildmat.2012.12.001
- Andrejkovičová, S., Velosa, A., Ferraz, E., Rocha, F.: Influence of clay minerals addition on mechanical properties of air lime metakaolin mortars. Constr. Build. Mater. 65, 132–139 (2014)
- Silva, A.S., Gameiro, A., Grilo, J., Veiga, R., Velosa, A.: Long-term behavior of lime–metakaolin pastes at ambient temperature and humid curing condition. Appl. Clay Sci. 88–89, 49–55 (2014). https://doi.org/10.1016/j.clay.2013.12.016
- Weise, K., Ukrainczyk, N., Koenders, E.: Pozzolanic reactions of metakaolin with calcium hydroxide: review on hydrate phase formations and effect of alkali hydroxides, carbonates and sulfates. Mater. Design 231, 112062 (2023). https://doi.org/10.1016/j.matdes.2023.112062
- Zunino, F., Scrivener, K.: The reaction between metakaolin and limestone and its effect in porosity refinement and mechanical properties. Cem. Concr. Res. 140, 106307 (2021)
- 45. Hewlett, P., Liska, M.: Lea's Chemistry of Cement and Concrete. Butterworth-Heinemann (2019)

- Mishra, J., Nanda, B., Patro, S.K., Krishna, R.: A comprehensive review on compressive strength and microstructure properties of ggbs-based geopolymer binder systems. Constr. Build. Mater. 417, 135242 (2024)
- 47. BS EN 196: Methods of Testing Cement. Accessed Jan. 2025
- Jones, B., Goos, P.: I-optimal versus d-optimal split-plot response surface designs. J. Qual. Technol. 44(2), 85–101 (2012)
- Payá, J., Monzó, J., Borrachero, M., Amahjour, F., Girbés, I., Velázquez, S., Ordóñez, L.: Advantages in the use of fly ashes in cements containing pozzolanic combustion residues: silica fume, sewage sludge ash, spent fluidized bed catalyst and rice husk ash. J. Chem. Tech. Biotech. 77(3), 331–335 (2002). https://doi.org/ 10.1002/jctb.583
- Sata, V., Jaturapitakkul, C., Kiattikomol, K.: Influence of pozzolan from various by-product materials on mechanical properties of high-strength concrete. Constr. Build. Mater. 21(7), 1589–1598 (2007). https://doi.org/10.1016/j.conbuildmat.2005.09.011
- Vimonsatit, S., Chindaprasirt, P., Ruangsiriyakul, S., Sata, V.: Influence of fly ash fineness on water requirement and shrinkage of blended cement mortars. KKU Eng. J. 42(4), 311–316 (2015). https://doi.org/10.14456/kkuenj.2015.37
- Sheng, G., Zhai, J., Li, Q., Li, F.: Utilization of fly ash coming from a cfbc boiler co-firing coal and petroleum coke in portland cement. Fuel 86(16), 2625–2631 (2007). https://doi.org/10.1016/j. fuel.2007.02.018
- Dvorkin, L., Zhitkovsky, V.: Cement-ash concrete with the addition of lime kiln dust. Front. Mater. 10, 1196407 (2023). https://doi.org/10.3389/fmats.2023.1196407
- Lanas, J., Sirera, R., Alvarez, J.I.: Study of the mechanical behavior of masonry repair lime-based mortars cured and exposed under different conditions. Cem. Concr. Res. 36(5), 961–970 (2006). https://doi.org/10.1016/j.cemconres.2005.12.003
- De Silva, P., Glasser, F.P.: Phase relations in the system cao al2o3 sio2 h2o relevant to metakaolin-calcium hydroxide hydration. Cem. Concr. Res. 23(3), 627–639 (1993)
- Appa Rao, G.: Generalization of abrams' law for cement mortars.
 Cement Concrete Res. 31, 495–502 (2001)
- Nagaraj, T., Banu, Z.: Generalization of abrams' law. Cem. Concr. Res. 26(6), 933–942 (1995)
- 58. Siddique, R., Klaus, J.: Influence of metakaolin on the properties of mortar and concrete: a review. Appl. Clay Sci. **43**(3–4), 392–400 (2009)
- Fortes-Revilla, C., Martínez-Ramírez, S., Blanco-Varela, M.T.: Modelling of slaked lime-metakaolin mortar engineering characteristics in terms of process variables. Cement Concr. Compos. 28(5), 458–467 (2006)
- Grilo, J., Silva, A.S., Faria, P., Gameiro, A., Veiga, R., Velosa, A.: Mechanical and mineralogical properties of natural hydraulic lime-metakaolin mortars in different curing conditions. Constr. Build. Mater. 51, 287–294 (2014)
- Rungchet, A., Chindaprasirt, P., Wansom, S., Pimraksa, K.: Hydrothermal synthesis of calcium sulfoaluminate-belite cement from industrial waste materials. J. Clean. Prod. 115, 273–283 (2016)
- Zhang, Y., Liu, J., Cheng, M., Li, Y., Huang, J., Jing, Z.: Hydrothermal solidification of underground construction wastes into building materials: waste slurry recycling, industrial application and evaluation. J. Clean. Prod. 426, 139091 (2023)
- Ergenç, D., Fort, R.: Accelerating carbonation in lime-based mortar in high co2 environments. Constr. Build. Mater. 188, 314–325 (2018)
- Cultrone, G., Sebastián, E., Huertas, M.O.: Forced and natural carbonation of lime-based mortars with and without additives: mineralogical and textural changes. Cem. Concr. Res. 35(12), 2278–2289 (2005)



- Rodriguez-Navarro, C., Ilić, T., Ruiz-Agudo, E., Elert, K.: Carbonation mechanisms and kinetics of lime-based binders: an overview. Cem. Concr. Res. 173, 107301 (2023)
- Antoni, M., Rossen, J., Martirena, F., Scrivener, K.: Cement substitution by a combination of metakaolin and limestone. Cem. Concr. Res. 42(12), 1579–1589 (2012)
- Vavričuk, A., Bokan-Bosiljkov, V., Kramar, S.: The influence of metakaolin on the properties of natural hydraulic lime-based grouts for historic masonry repair. Constr. Build. Mater. 172, 706–716 (2018)
- De Weerdt, K., Haha, M.B., Le Saout, G., Kjellsen, K.O., Justnes, H., Lothenbach, B.: Hydration mechanisms of ternary portland cements containing limestone powder and fly ash. Cem. Concr. Res. 41(3), 279–291 (2011)
- Tironi, A., Castellano, C.C., Bonavetti, V.L., Trezza, M.A., Scian, A.N., Irassar, E.F.: Kaolinitic calcined clays-portland cement system: hydration and properties. Constr. Build. Mater. 64, 215–221 (2014)
- Zeng, Q., Li, K., Fen-Chong, T., Dangla, P.: Pore structure characterization of cement pastes blended with high-volume fly ash. Cem. Concr. Res. 42(1), 194–204 (2012). https://doi.org/10.1016/j.cemconres.2011.09.003
- Liu, M., Gadikota, G.: Phase evolution and textural changes during the direct conversion and storage of co2 to produce calcium carbonate from calcium hydroxide. Geosciences 8(12), 445 (2018)

Publisher's Note Springer Nature remains neutral with regard to jurisdictional claims in published maps and institutional affiliations.

